

Numerical Study on Space-Time Pulse Compression

Monika Pietrzyk

*Institute of Fundamental Technological Research
Polish Academy of Sciences
Świętokrzyska 21, 00-049 Warsaw, Poland*

Abstract

A numerical study of the properties of Gaussian pulses propagating in planar waveguide under the combined effect of positive Kerr-type nonlinearity, diffraction in planar waveguides and anomalous or normal dispersion, is presented. It is demonstrated how the relative strength of dispersion and diffraction, the strength of nonlinearity and the initial spatial and temporal pulse chirps effect on the parameters of pulse compression, such as the maximal compression factor and the distance to the point of maximal compression.

1 Introduction

A compression of optical pulses in Kerr-type nonlinear media have been subject to investigation for many years and continues to attract a certain attention [1, 2]. In single-mode fibers with anomalous group-velocity dispersion (GVD) and positive nonlinearity the pulse compression is based on the mechanism of higher-order soliton generation [3]. In single-mode fibers with normal GVD the pulse compression can be obtained in the configuration with a grating pair [4, 5]. In both cases the self-phase modulation (SPM) induced by an intense pulse is used. However, the intense pump pulse propagating together with a weak probe pulse can also cause pulse compression by the mechanisms of the so-called cross-phase modulation (XPM) [6], or the induced-phase modulation (IPM) [7].

A possibility of pulse compression in non-dispersive nonlinear bulk media due to another nonlinear effect, that of self-focusing, is discussed in [8]-[10] with the aid of the paraxial ray approximation, [8, 10], and by means of the variational analysis, [9]. Still another pulse compression technique that uses the self confinement of two-dimensional spatial bright solitons propagating in non-dispersive bulk media is mentioned in [11], where the two-beam interference technique is used in order to ensure that a filamentation (a splitting of the beam into many sub-beams) does not occur.

Moreover, a simultaneous space-time collapse, which can occur in bulk media and in planar waveguides under the combined effect of nonlinearity, diffraction and anomalous dispersion, may also be useful for pulse compression [12, 13]. This kind of collapse gives rise to short pulses with extremely high optical field [14, 15, 16]. It is realizable both in the case when dispersion and diffraction have comparable effect on pulse propagation and in the more general case when one of the effects above is dominating (see [17]).

On the other side, the interplay of normal dispersion and positive nonlinearity causes quite different behavior of the pulse. In optical fibers where diffraction terms are not included it leads to a monotonic pulse spreading. However, the inclusion of the diffraction term, which is necessary for a planar waveguide, can lead to a pulse compression, as it was described in [17, 18]. Besides, in planar waveguide, normal dispersion slows the self-focusing of the pulse and causes a splitting of the pulse into two pulses [18, 19]. The effect of splitting of a pulse was observed also in the bulk media [12].

In this paper a compression of a pulse propagating in planar, self-focusing nonlinear planar waveguide in the regime of anomalous and normal dispersion is considered. The structure of the paper is as follows. In Section 2, the nonlinear Schrödinger equation describing dispersive pulse propagation in nonlinear planar waveguides and the parameters of pulse compression are introduced. In Section 3, an estimation of the

condition of pulse collapse is made with the aid of the so-called method of moments [20]. Numerical results describing the influence of the magnitude of nonlinearity, the relative strength of dispersion and diffraction and the spatial and temporal chirp of the initial Gaussian pulse on the pulse compression parameters are discussed in Section 4.

2 Basic equations

It is well known that starting from the Maxwell equations for the envelope $U(x, y, z, t)$ of the electric field

$$E(x, y, z, t) = U(x, y, z, t)e^{-i(\omega t - n_0 \beta_0 z)}$$

propagating along the z axis in a planar waveguide with positive, instantaneous Kerr-type nonlinearity, one obtains the 2-dimensional nonlinear Schrödinger equation (NSE) [18] :

$$i \frac{\partial}{\partial \zeta} U - \frac{1}{2} \sigma \frac{\partial^2}{\partial \tau^2} U + \frac{1}{2} \frac{\partial^2}{\partial \xi^2} U + N^2 |U|^2 U = 0, \quad (1)$$

if the paraxial and the slowly varying envelope approximations are applied and the term $\nabla \cdot (\nabla E)$, the shock term [21] proportional to $\frac{\partial(|E|^2 E)}{\partial t}$ and higher-order dispersion effects can be neglected.

In Equation 1, $\zeta = \frac{z}{z_f}$ is the normalized longitudinal spatial coordinate, $\xi = \frac{x}{w_0}$ is the normalized transverse spatial coordinate, $\tau = \frac{t - \beta_1 z}{t_0}$ is the normalized local time, $\sigma = \frac{\beta_2 z_f}{t_0^2}$ represents the relative strength of dispersion and diffraction, $N = \beta_0 U_0 w_0 \sqrt{n_0 n_2}$ parameterizes the strength of nonlinearity, $\beta_0 = \frac{\omega}{c}$ is a wave number, $\beta_n = \frac{d^n \beta}{d \omega^n}$ are dispersion terms, $z_f = \beta_0 n_0 w_0^2$ is the Fresnel diffraction length, w_0 is the spatial width of the input pulse, t_0 is the temporal width of the input pulse (i.e., duration of the input pulse), U_0 is the peak amplitude of the input pulse, and $n = n_0 + n_2 |U|^2$ is the refraction index for the Kerr type nonlinear media. Recall that $\sigma > 0$ corresponds to the normal dispersion and $\sigma < 0$ corresponds to the anomalous dispersion.

As the initial condition we take the Gaussian chirped pulse which is given by (cf. [22])

$$U(\xi, \tau, \zeta = 0) = e^{-\frac{\xi^2(1+iC_\xi)}{2}} e^{-\frac{\tau^2(1+iC_\tau)}{2}}, \quad (2)$$

where C_ξ (C_τ) is the spatial (temporal) pulse chirp (the focusing spatial chirp corresponds to $C_\xi < 0$ and the focusing temporal chirp corresponds to $\text{sgn}(-\sigma C_\tau) < 0$).

We will characterize a pulse by its spatial width, $w_\xi(\zeta)$, and the temporal width, $w_\tau(\zeta)$, which are defined by

$$U(w_\xi, 0, \zeta) = \frac{1}{e}U(0, 0, \zeta) \quad \text{and} \quad U(0, w_\tau, \zeta) = \frac{1}{e}U(0, 0, \zeta).$$

We also introduce the maximal compression factor

$$c_{max} = \frac{\tau_0}{w_{\tau min}(\zeta_m)},$$

where $w_{\tau min}(\zeta_m)$ is the minimal temporal width of the pulse (see [18, 23]). In following we call ζ_m the position of the minimal pulse width.

Solution of NSE (Equation 1) with the initial condition given by Equation 2 can describe a propagation of a dispersive Gaussian pulse in nonlinear planar waveguides. It is worth remarking that for the anomalous dispersion regime a solutions of this equation can also describe a dispersion-less elliptic Gaussian beam, [24, 25] (i.e. a cw beam with elliptic Gaussian transverse profile) propagating in a nonlinear bulk media.

In this paper we refer to the case of $\sigma = -1$ as the cylindrically symmetric spatiotemporal pulse; the case of $\sigma \neq -1$ is to be referred to as the asymmetric spatiotemporal pulse.

In the particular case of the cylindrical spatiotemporal pulse a simple analytic solution of the NSE exists which describes a behavior of beam propagating in nonlinear media by means of the variational approximation [14] or by means of the scaled complex rays formulation within the so-called ABCD matrix formalism (see [26, 27]). For the asymmetric spatiotemporal pulse only a semi-analytical approach of [24, 25] is known in the literature.

It is known that some solutions of the two- or three-dimensional NSE can develop into a singularity of the electric field when the initial pulse power exceeds a certain critical value [14]. This phenomenon, known as a pulse collapse, can occur simultaneously in space and time for a pulse propagating in planar waveguide with the anomalous GVD [14, 15], and also for a dispersion-less beam propagating in self-focusing bulk medium. This singularity, however, is obviously non-physical, for it emerges just as an artifact of the paraxial approximation made when deriving the NSE. In order to avoid this limitation, either a non-paraxial treatment of the process of self-focusing [28] or some other effects, such as the nonlinear absorption and the saturation of the nonlinear refractive index, should be taken into consideration. From another hand, the appearance of a non-physical singularity in numerical simulations based on NSE can serve as an indication to the real collapse taking place in the certain point of space. This is in fact the criterion used in Section 4.

Studying the details of developing the pulse collapse we leave beyond the scope of this paper. Instead, our task is to determine the values of the parameters σ and

N^2 for which the pulse collapse can occur. For this purpose the so-called method of moments [29] could be used. However, it gives only an estimation of the sufficient conditions of the pulse collapse, whereas the latter can occur, in fact, at the earlier times or on the shorter propagation distances [10]. More precise conditions will be obtained by means of the numerical simulations presented in Section 3, (cf. also [14])

3 Sufficient conditions of pulse collapse

The method of moments originates from the paper of Vlasov e.a. [29]. It can be used as an approach to the determination of whether a given initial wave pulse can collapse to a singular point in a finite period of time [30]. An application of the method of moments to the NSE may be found in [20].

In order to formulate the condition of collapse in terms of the strength of non-linearity, N^2 , and the relative strength of dispersion and diffraction, σ , we first introduce the second moment of intensity

$$I(\zeta) = \int_{-\infty}^{\infty} \int_{-\infty}^{\infty} (\xi^2 + \bar{\tau}^2) |U|^2 d\xi d\bar{\tau},$$

where U is a solution of the NSE given by Equation 1, with the normalization $\bar{\tau} = (-\sigma)^{-\frac{1}{2}} \tau$, ($\sigma \neq 0$).

Parameter I can be interpreted as effective beam size measuring the size of the area to which most of the energy is confined.

Assuming that U decay suitably as $r \rightarrow \infty$, one can obtain [20]

$$\frac{d^2 I}{d\zeta^2} = \ddot{I} = 4E \quad (3)$$

where E is the Hamiltonian of the NSE

$$E = \int \int \left(\frac{1}{2} \left| \frac{\partial U(\xi, \bar{\tau})}{\partial \xi} \right|^2 + \frac{1}{2} \left| \frac{\partial U(\xi, \bar{\tau})}{\partial \bar{\tau}} \right|^2 - \frac{1}{2} N^2 |U(\xi, \bar{\tau})|^4 \right) d\xi d\bar{\tau}$$

Because E remains constant during a pulse propagation, i.e. it is independent of ζ , Equation 3 may be integrated twice to give :

$$I(\zeta) = 2E\zeta^2 + \dot{I}(0)\zeta + I(0),$$

where $\dot{I} = \frac{dI}{d\zeta}$.

If the right-hand side of the above equation vanished, then the pulse width (both spatial and temporal) will decrease to zero in a finite distance leading to beam collapse. Therefore a sufficient condition for collapse can occur if the following conditions are satisfied [20, 22, 30]:

$$\begin{aligned} E &< 0 \quad , \\ E &= 0 \quad \text{and} \quad \dot{I}(0) < 0, \\ E &> 0 \quad \text{and} \quad \dot{I}(0) < -\sqrt{8EI(0)}. \end{aligned} \tag{4}$$

For Gaussian input pulse, given by Equation 2, Hamiltonian E can be expressed in the following form

$$E = \frac{1}{2} \int \int [(\xi^2 - \sigma^2 \bar{\tau}^2) e^{-\xi^2} e^{-\sigma \bar{\tau}^2} - N^2 e^{-2\xi^2} e^{-2\sigma \bar{\tau}^2}] d\xi d\bar{\tau} = \frac{1}{4} \sqrt{-\sigma} \pi (1 - \sigma - N^2).$$

In the particular case of flat phase front, $C_\xi = C_\tau = 0$, we obtain that $\dot{I}(0) = 0$ and because of this two last criterion in Equation 4 are not satisfied. The first criterion, $E < 0$, yields

$$N^2 > 1 - \sigma. \tag{5}$$

Equation 5 may be considered as the sufficient condition of the pulse collapse in terms of the strength of nonlinearity, N^2 , which is proportional to the peak amplitude, $|U_0|^2$, and the relative strength of dispersion and diffraction, σ . The magnitude of the parameter N^2 which is sufficient for the pulse collapse to occur increases linearly with $|\sigma|$. This is not unexpected because the collapse of the pulse occurs when the self-focusing caused by the nonlinearity dominates over the broadening of a pulse, which is due to the diffraction and dispersion. It is obvious that for smaller values of the parameter $|\sigma|$ is, the influence of the dispersion on the pulse broadening is weaker.

Note that the sufficient conditions of pulse collapse can be formulated also in terms of the critical initial power P_c of the pulse as follows [22, 25]

$$\frac{P_c}{P_0} = \left[\sqrt{|\sigma|} + \frac{1}{\sqrt{|\sigma|}} \right] \geq 1,$$

where $P_c(\sigma) = \int |U|^2 d\bar{\tau} d\xi = \pi |U_0|^2 \frac{1}{\sqrt{|\sigma|}}$, $P_0 = 2\pi$ is the initial power of the cylindrically symmetric pulse (i.e. $\sigma = 1$).

We conclude that the decrease of the parameter $|\sigma|$ leads to the decrease of the critical amplitude, $|U_0|^2$, and to the increase of the critical power, P_c .

Note, that the collapse criteria obtained with the aid of the method of moments for the particular case of the spatiotemporal symmetric pulse agrees with the result of the variational approximation in [10, 14].

4 Numerical results and discussion

In this Section, the results of numerical solution of the 2+1 dimensional NSE by means of the well-known Split-Step Spectral Method (SSSM) [31] with the two dimensional (2d) Fast Fourier Transform [32] are presented. The calculations on the two-dimensional grid with 512×512 points (transverse steps, $\Delta\xi = \Delta\tau = 0.08$) and with the longitudinal step depending on the nonlinearity so that for $N^2 = 1$, $\Delta\zeta = 0.01$, were performed. Because of the lack of spatial-temporal cylindrical symmetry of the problem it is not possible to simplify calculations by reducing the 2d Fast Fourier Transform to the one dimensional Hankel Transform developed in [33, 34]. Several checks of our numerical procedure were made, which include a simulation of beam propagation in the absence of group-velocity dispersion ($\sigma = 0$), repeated testing with different transverse grid and longitudinal step length, and the monitoring of pulse energy during each simulation. The latter was kept constant with an error < 0.00005

As initial conditions in numerical calculations we take Gaussian pulse given by Equation 2. First, for the case of anomalous dispersion regime we will compare conditions of pulse collapse predicted by method of moments with those obtained from numerical calculations. Further, with the aid of numerical calculations we will study influence of the strength of nonlinearity, relative strength of dispersion and diffraction and spatial and temporal pulse chirps on pulse compression parameters. Above analysis will be perform both for anomalous as well as normal dispersion regime.

4.1 The anomalous dispersion regime

In this section the influence of the parameters σ and N^2 on the pulse collapse and compression will be considered.

In Fig. 1, a comparison of the conditions of the collapse of pulse predicted by the method of moments with those obtained by numerical calculations is presented. In our numerical procedure the occurrence of pulse collapse was identified with the discontinuity of the phase $\phi(0, 0, \zeta)$ in the central point of the pulse $u = |u|e^{i\phi}$, and with a non-monotonic behavior of the intensity in the central point of the pulse after reaching the collapse point. The results of numerical simulation are plotted by two kinds of points corresponding to the cases when, respectively, the pulse collapse occurs or does not occur. The prediction of the method of moments is given by the straight line $N^2 = 1 - \sigma$, (see Equation 5). The boundary line between the collapse and the no collapse regions, obtained from the numerical data is approximately described by $N^2 \approx 0.85 - \sigma$. It is parallel to the straight line predicted by the method of moments, unless the absolute value of σ is too small.

Therefore, for both methods, the magnitude of the parameter N^2 which is sufficient for the pulse collapse to occur increase linearly with $|\sigma|$. The discrepancy appears due to the theoretical idealization of the picture of the collapse where all the energy of the pulse goes to the singularity point. This also explains why conditions of numerical collapse are typically softer than those predicted by the method of moments described in Section 3.

Studying details of pulse collapse we leave beyond task of this paper. Instead, we will study the influence of the relative strength of dispersion and diffraction, the nonlinearity and the spatial and temporal chirps on the parameters of pulse compression under the condition that the pulse collapse does not occur.

Fig. 2 and Fig. 3 represent the results of calculations of the influence of the relative strength of dispersion and diffraction, σ , on the maximal compression factor, c_{max} , and on the position of the minimal pulse width, ζ_m , for different values of the strength of nonlinearity, N^2 and for Gaussian initial pulse with flat phase front. As it could be expected the parameters of pulse compression, c_{max} and ζ_m , increase monotonically with the increase of N^2 and the decrease of σ until collapse conditions are reached. This behavior is obvious from the fact that increase of N^2 cause increase of pulse self-focusing, it helps to concentrate pulse energy in the center, in addition, decrease of σ cause decrease of dispersion broadening of the pulse.

In Fig. 4 the results of numerical simulations of the influence of the initial spatial, $C_\xi = C$, and two cases of temporal, $C_\tau = \pm C$, chirps on the pulse compression parameters are presented. In order to distinguish between the above two cases we introduce a parameter

$$S = \text{sgn}(-C_\xi C_\tau \sigma),$$

which equals 1 for the case of focusing (defocusing) temporal and spatial chirps and equals -1 for the case of focusing (defocusing) temporal and defocusing (focusing) spatial chirps.

As it could be expected, the focusing spatial and temporal chirps, $C < 0, S = 1$, cause the increase of the pulse compression parameters. The explanation is that a defocusing chirp spreads the energy out from the center of the pulse, whereas a focusing chirp concentrates it there. As the result, the nonlinearity-induced phase curvature of the field is, respectively, reduced or enhanced. Similar effect of the focusing chirp of the initial pulse takes place in the region close to the collapse. Namely, the focusing spatial chirp can hasten the collapse, whereas a defocusing chirp can either delay or eliminate it entirely [17].

More interesting is the case of $S = -1$ (i.e. the spatial focusing chirp and the temporal defocusing chirp occur simultaneously). The increase of the maximal compression factor occurs only for the case of focusing temporal chirp, $C > 0$, whereas this is not always true for a spatial focusing chirp $C < 0$, see Fig. 4. One can conclude that the temporal chirp has larger effect on the temporal pulse

compression than the spatial one. One can expect the reverse situation in the case of spatial compression of the pulse.

4.2 Normal dispersion regime

In the case of normal dispersion regime the collapse of the pulse doesn't occur. However, due to the spatiotemporal coupling occurring in nonlinear medium when both the diffraction and the dispersion effects take place a pulse compression can be obtained [18].

In this section we will study the influence of the relative strength of dispersion and diffraction, the nonlinearity and the spatial and temporal pulse chirps on the parameters of pulse compression.

It is seen from Fig. 5 that the maximal compression factor, c_{max} , monotonically decreases with σ , and increases with N^2 . It is clear because smaller value of the parameter σ has a weaker influence on the dispersion broadening of the pulse, moreover the increase of N^2 leads to the increase of the spatiotemporal coupling and nonlinearity induced phase curvature of the field. In the end both effects lead to the temporal compression of the pulse.

From Fig. 6 it is seen that for sufficiently small values of σ the parameter ζ_m decreases with N^2 . However it appears to be practically independent on σ once a certain threshold level of N^2 is reached. This fact was explained in [17] by means of the periodic beam narrowing of higher-order spatial solitons. A different behavior takes place at larger values of σ ($\sigma > 0.25$). Namely, at first ζ_m increases with N^2 for sufficiently small N^2 and then it slowly decreases after reaching a maximal value at the certain value of N^2 . This behavior is explainable by the fact that at small nonlinearities the effects of dispersion prevent a creation of spatial solitons.

In Fig. 7 the results of numerical calculations of the influence of the initial pulse chirp on the parameters of pulse compression c_m and ζ_m are presented. The focusing spatial and temporal chirps, $C < 0, S = 1$, cause the increase of the compression parameters (c_{max} and ζ_{max}) and this behavior appears to be similar to that which we have previously observed in Fig. 4 for the anomalous dispersion regime. However, in the case of the anomalous GVD c_{max} grows with C much faster than in the case of normal GVD. Namely, for the anomalous GVD the maximal compression factor for a chirped initial pulse with $C = -2$ is three times larger than that for an initial pulse with flat phase front ($C = 0$, i.e. $c_{max}(C = -2) = 3 \times c_{max}(C = 0)$). For the normal GVD the increase of the c_{max} is rather slow, e.g. $c_{max}(C = -2) = 1.1 \times c_{max}(C = 0)$, and a saturation of the maximal compression factor occurs for the initial chirps below -2 (see Fig. 7).

Moreover, for the case of $C < 0, S = -1$ (i.e. the spatial focusing chirp and the temporal defocusing chirp) the maximal compression factor increases only for

focusing temporal chirp, whereas this is not always true for a spatial focusing chirp $C_\xi < 0$.

5 Conclusions

In this paper, the physical conditions of collapse and compression of dispersive Gaussian pulses propagating in waveguide with the positive Kerr-type nonlinearity, diffraction and the anomalous or normal dispersion are investigated.

We determine the values of the relative strength of dispersion and diffraction, σ , and the strength of nonlinearity, N^2 , for which the pulse collapse can occur. For this purpose we first present an estimation given by the method of moments [29]. More precise conditions are obtained by means of the numerical simulations based on the (2+1)-dimensional Nonlinear Schrödinger Equation (see Section 4).

We characterize a pulse compression by two parameters: the maximal compression factor, c_{max} , and the distance to the point of the maximal compression, ζ_m , (see Section 2). By means of a numerical simulation we study how these two parameters depend on the parameters N^2 and σ , and the initial spatial and temporal pulse chirps. We demonstrate that in the regime of both anomalous and normal dispersion the increase of the nonlinearity and the decrease of the relative strength of dispersion and diffraction cause the increase of the maximal compression factor. Moreover, in the case of anomalous dispersion regime the compression factor is maximal in the region of $1 - \sigma \lesssim N^2$.

Furthermore, we observe that the increase of the focusing temporal and spatial chirps of the initial pulse lead to the increase of the maximal compression factor, c_{max} . In the case of the anomalous GVD c_{max} grows with chirp, C , much faster than in the case of normal GVD, for which a saturation of the maximal compression factor occurs.

Moreover, the increase of the focusing temporal chirp might lead, even in the presence of the defocusing spatial chirp, to the increase of the maximal compression factor, c_{max} , whereas the defocusing temporal chirp always leads to the decrease of c_{max} , even in the case of the focusing spatial chirp. It may be concluded, therefore, that the temporal chirp has larger effect on the maximal pulse compression factor than the spatial chirp. In reverse, it is expected that the spatial focusing chirp has larger impact on the beam width than the temporal chirp, independently on its sign.

6 Acknowledgments

I would like to thank I. Kanatchikov for his helpful suggestions.

References

- [1] K. Tamura, M. Nakazawa, *Opt. Lett.* **21** (1996) 68
- [2] K. C. Chan, H. F. Liu, *IEEE J. Quantum Electron.* **31** (1995) 2226
- [3] K. C. Chan, H. F. Liu, *Opt. Lett.* **19** (1994) 49.
- [4] R. F. X. A. M. Mols, G. J. Ernst, *Opt. Comm.* **94** (1992) 509.
- [5] A. M. Weiner, J. P. Heritage, R. H. Stolen, *J. Opt. Soc. Am. B* **5** (1988) 364.
- [6] G. P. Agrawal, P.L. Baldeck, R. R. Alfano, *Opt. Lett.* **14** (1989) 137.
- [7] M. Jamashita, K. Torizuka, *Jap. J. of Appl. Phys.* **29** (1990) 294.
- [8] J. T. Manassah, P. L. Baldeck, R.R. Alfano, *Opt. Lett.* **13** (1988) 1090.
- [9] M. Karlsson, D. Anderson, M. Desaix, M. Lisak, *Opt. Lett.* **16** (1991) 1373.
- [10] J. T. Manassah, B. Gross, *Opt. Lett.* **17** (1992) 976.
- [11] D. H. Reitze, A. M. Weiner, D. E. Leaird, *Opt. Lett.* **16** (1991) 1409.
- [12] P. Chernev, V. Petrov, *Opt. Lett.* **17** (1992) 172.
- [13] S. K. Turisyn, *Phys. Rev. A* **47** (1992) 27.
- [14] M. Desaix, D. Anderson, M. Lisak, *J. Opt. Soc. Am. B* **8** (1991) 2082.
- [15] Y. Silberger, *Opt. Lett.* **15** (1990) 1282.
- [16] J. T. Manassah, *Opt. Lett.* **16** (1991) 563.
- [17] A. T. Ryan, G. P. Agrawal, *J. Opt. Soc. Am. B* **12** (1995) 2382.
- [18] A. T. Ryan, G. P. Agrawal, *Opt. Lett.* **20** (1995) 306.
- [19] D. Burak, R. Binder, *Proc. of Quantum Electr. and Laser Science Conf., Anaheim, California, June 2-7, 1996, QPD12-1.*
- [20] F. H. Berkshire, J. D. Gibbon, *Stud. in Appl. Math.* **69** (1983) 229.
- [21] J. E. Rothenberg, *Opt. Lett.* **17** (1992) 583.
- [22] X. D. Cao, G. P. Agrawal, C. J. McKinstrie, *Phys. Rev. A* **49** (1994) 4085.

- [23] R. F. X. A. M. Mols, G. J. Ernst, *Opt. Comm.* **94** (1992) 509.
15, 1005 (1965)
- [24] V. Magni, G. Cerullo, S. De Silvestri, A. Monguzzi, *J. Opt. Soc. Am .B* **12** (1995) 476.
- [25] F. Cornolti, M. Lucchesi, B. Zambon, *Opt. Comm.* **75** (1990) 129.
- [26] W. Nasalski, *Opt. Appl.* **XXIV** (1994) 4.
- [27] W. Nasalski, *Optics Comm.* **119** (1995) 218.
- [28] M. D. Feit, J. A. Fleck, Jr, *J. Opt .Soc .Am. B* **5** (1988) 633.
- [29] S. N. Vlasov, V. A. Petrishchev, V. I. Talanov, *Izv. Vuz Radiofiz*, **14** (1971) 1353.
- [30] J. J. Rasmussen, K. Rypdal, *Phys. Scripta* **33** (1986) 481.
- [31] G. P. Agrawal, "Nonlinear Fiber Optics," Academic Press, Boston (1989)
- [32] "Numerical Recipes in Fortran," W. H. Press, Cambridge Press (1992)
- [33] A. E. Siegman, *Opt. Lett.* **1** (1977) 13.
- [34] M. Van Veldhuizen, R. Nieuwenhuizen, W. Zijl, *J. of Comp. Phys.* **110** (1994) 196.
- [35] G. Fibich, V. M. Malkin, G. C. Papanicolaou, *Phys. Rev. A.* **52** (1995) 4218.
- [36] V. Vysloukh, T. Matveeva, *Bull. Russ. Acad. Sci. Phys.* **56** (1992) 1289.

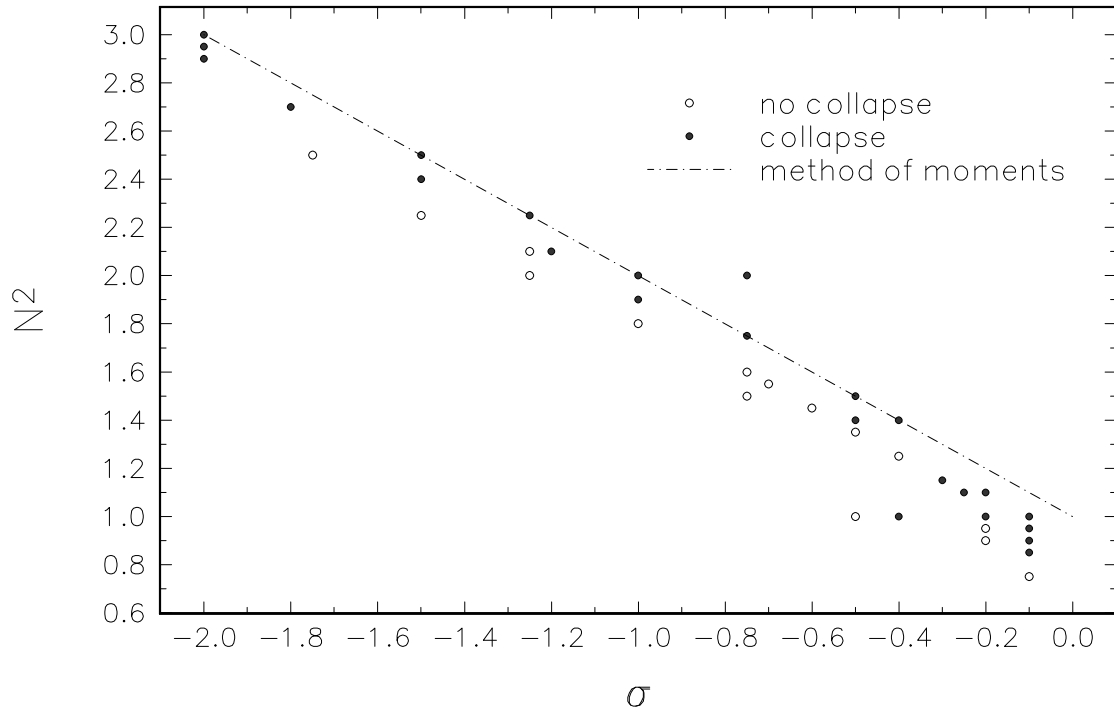


Figure 1: Comparison of the sufficient conditions for pulse collapse predicted by the method of moments (straight line) and numerical calculations (filled circle points denote pulse collapse and empty circle points indicate no collapse). It was done for initial Gaussian pulse with flat phase front, propagating in a medium described by two parameters: the strength of the nonlinearity, N^2 and the relative strength of dispersion and diffraction, σ .

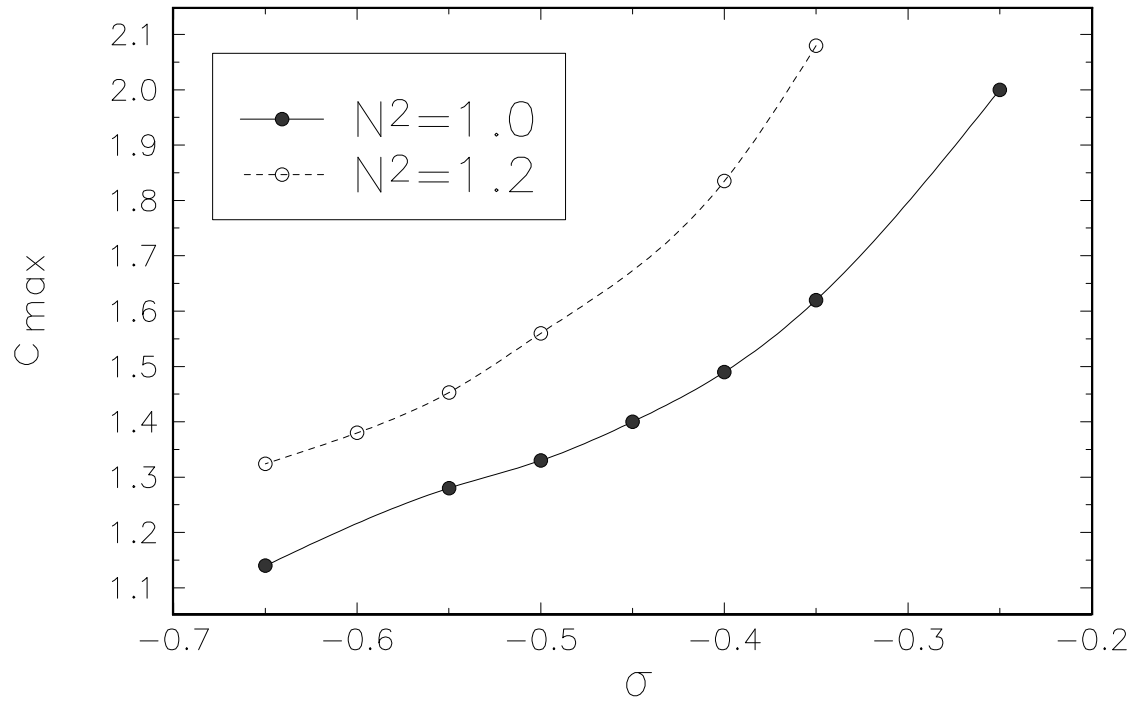


Figure 2: The maximum compression ratio, c_{max} as a function of the relative strength of dispersion and diffraction, $\sigma < 0$, for different value of the strength of nonlinearity, N^2 , and for initial Gaussian pulse with flat phase front.

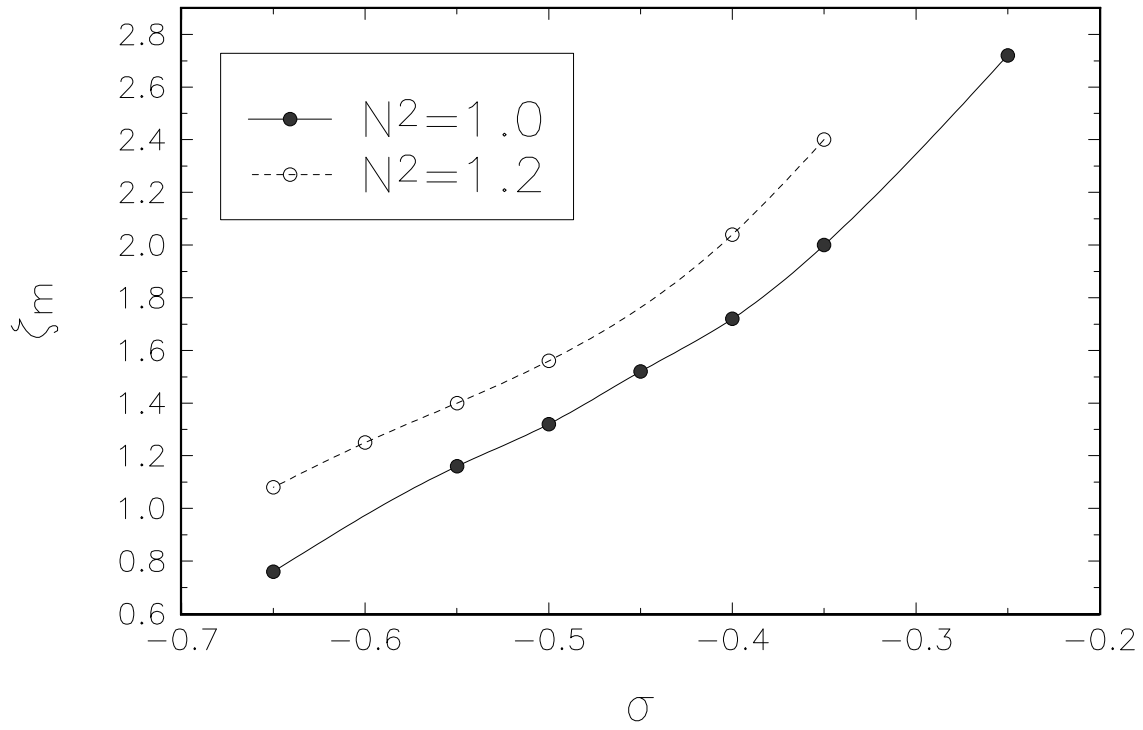


Figure 3: The distance to the point of minimal pulse width, ζ_m , as a function of the relative strength of dispersion and diffraction, $\sigma < 0$, for different value of the strength of nonlinearity, N^2 , and for initial Gaussian pulse with flat phase front.

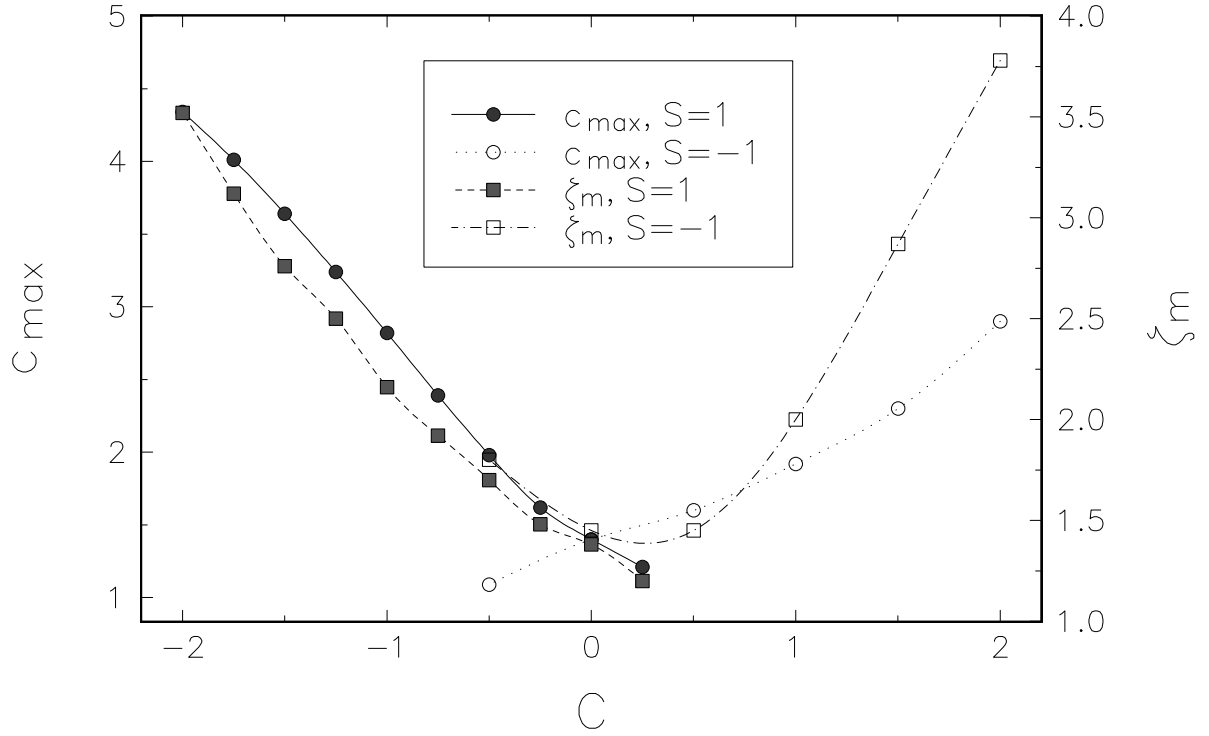


Figure 4: The maximal compression factor, c_{max} , and the distance to the point of the minimal pulse width, ζ_m , as a function of the initial spatial and temporal pulse chirps, $C_\xi = C$ and $C_\tau = \pm C$, respectively. Spatial focusing chirp occurs for $C < 0$, temporal focusing chirp occurs for $C_\tau < 0$, $\sigma = -0.5$ and $N^2 = 1.0$.

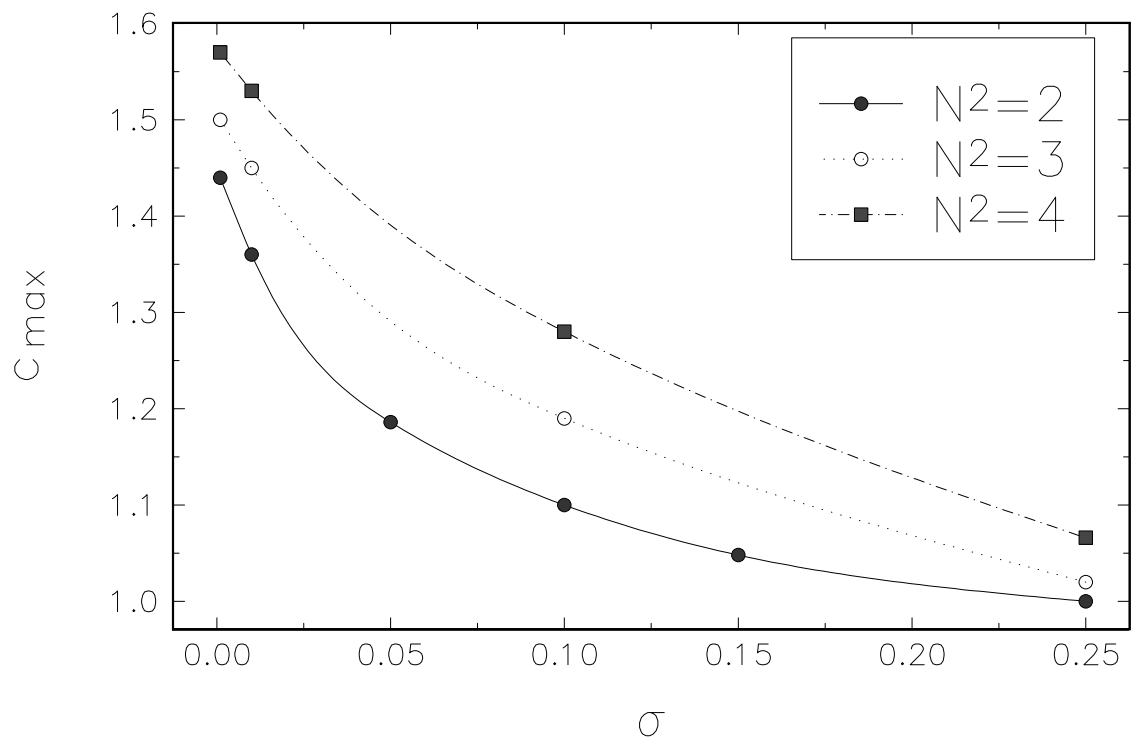


Figure 5: The maximal compression factor, c_{max} , as a function of the relative strength of dispersion and diffraction, $\sigma > 0$, for different value of the strength of nonlinearity, N^2 , and for initial Gaussian pulse with flat phase front.

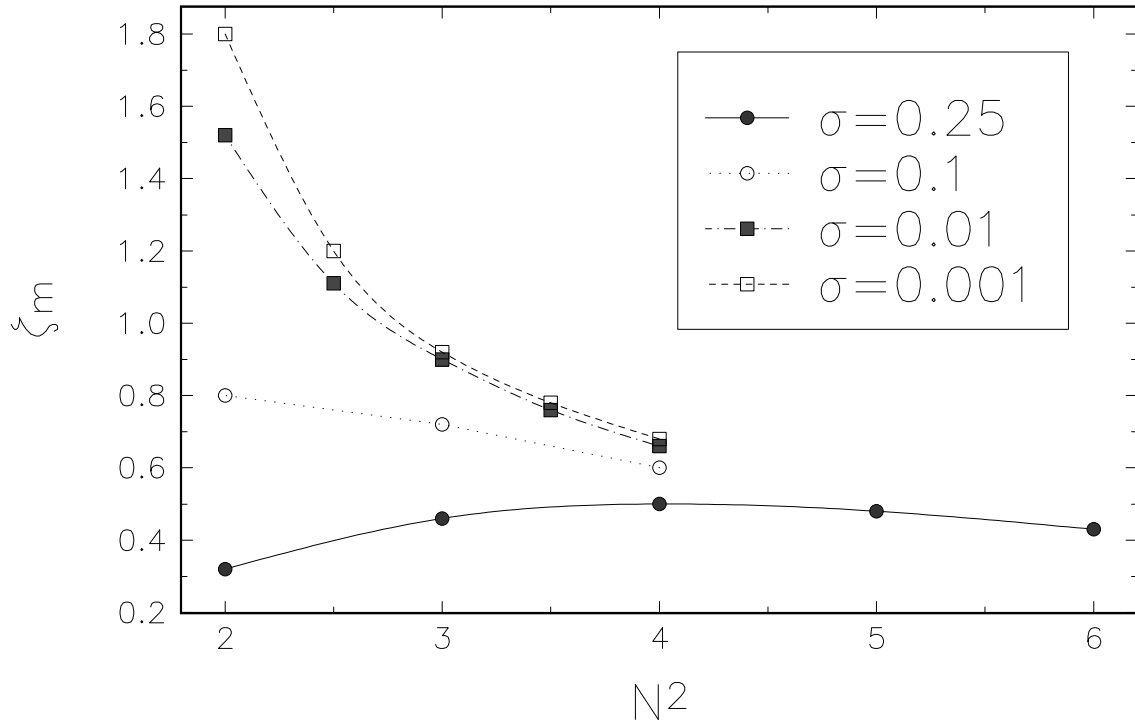


Figure 6: The distance to the point of the minimal pulse width, ζ_m , as a function of the strength of nonlinearity, N^2 , for different value of the relative strength of dispersion and diffraction, $\sigma > 0$, and for initial Gaussian pulse with flat phase front.

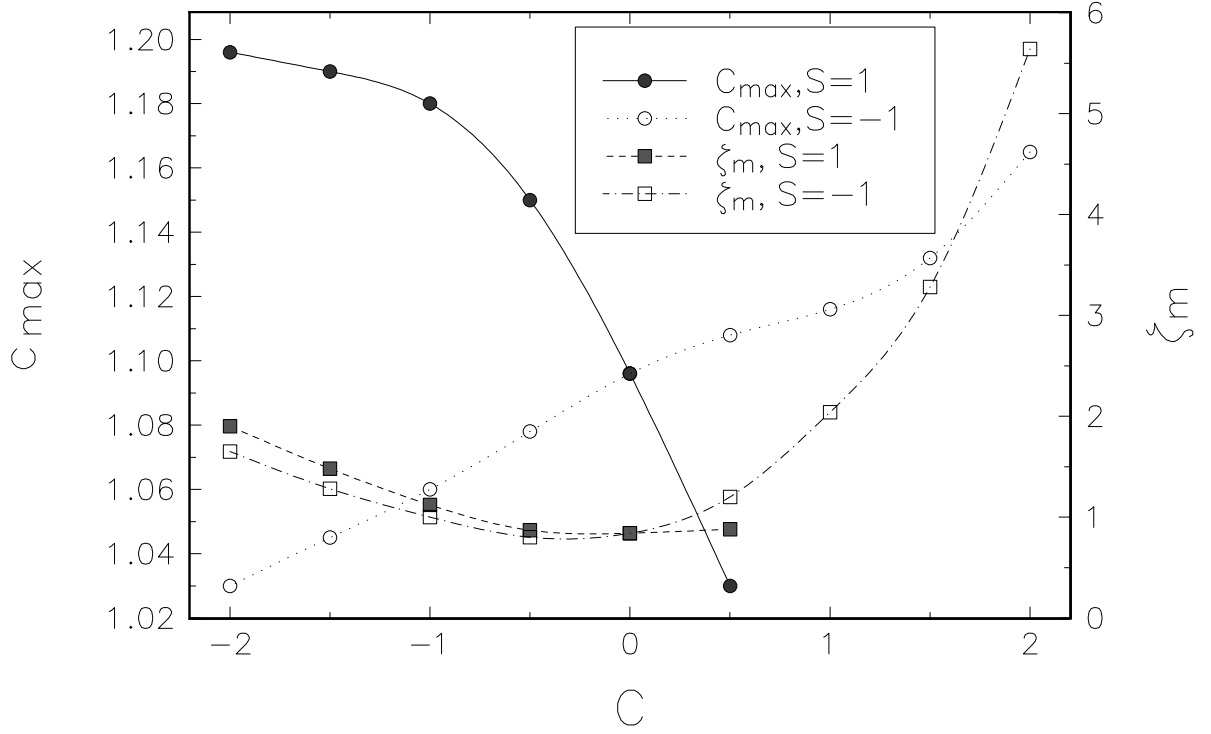


Figure 7: The maximal compression factor, c_{max} , and the distance to the point of the minimal pulse width, ζ_m , as a function of the initial spatial and temporal pulse chirps, $C_\xi = C$ and $C_\tau = \pm C$, respectively. Spatial focusing chirp occurs for $C_\xi < 0$, temporal focusing chirp occurs for $C_\tau > 0$, $\sigma = 0.1$ and $N^2 = 2.0$.